

ChemComm

Accepted Manuscript



This is an *Accepted Manuscript*, which has been through the Royal Society of Chemistry peer review process and has been accepted for publication.

Accepted Manuscripts are published online shortly after acceptance, before technical editing, formatting and proof reading. Using this free service, authors can make their results available to the community, in citable form, before we publish the edited article. We will replace this *Accepted Manuscript* with the edited and formatted *Advance Article* as soon as it is available.

You can find more information about *Accepted Manuscripts* in the [Information for Authors](#).

Please note that technical editing may introduce minor changes to the text and/or graphics, which may alter content. The journal's standard [Terms & Conditions](#) and the [Ethical guidelines](#) still apply. In no event shall the Royal Society of Chemistry be held responsible for any errors or omissions in this *Accepted Manuscript* or any consequences arising from the use of any information it contains.

Cite this: DOI: 10.1039/c0xx00000x

www.rsc.org/xxxxxx

ARTICLE TYPE

Intrinsic magnetic characteristics dependent charge transfer and visible photo-catalytic H₂ evolution reaction (HER) properties of Fe₃O₄@PPy@Pt catalyst

Wenyan Zhang^{a,b,c}, Chao Kong^{a,b}, Wei Gao^{a,b}, Gongxuan Lu^{a*}

5 Received (in XXX, XXX) Xth XXXXXXXXXX 20XX, Accepted Xth XXXXXXXXXX 20XX

A ternary nano-architectural photocatalyst has been designed to investigate whether the intrinsic magnetic property of photo-catalysts have effect on the charge transfer and its photo-catalytic H₂ evolution reaction (HER) properties under visible light irradiation. The electron transfer and the visible-light-driven hydrogen evolution were remarkably enhanced by regulating the electro-magnetic interaction between the magnetic catalysts and the photo-generated electrons.

15 With the improvement of society, it is urgent to search for efficient, clean and renewable energy resource to solve the energy crisis caused by over-consuming fossil fuel and accompanied environmental pollutions¹. Hydrogen has been acknowledged as an ideal sustainable energy for the future because of its higher combustion enthalpy than conventional fuels and "zero-pollution" (avoiding the production of greenhouse gases)². Splitting water by solar energy is a promising strategy for hydrogen generation.³ Plenty of advances have been reported to enhance the efficiency of visible-light-driven H₂ evolution, including the application of high active catalysts, improving the charge separation by the aids of carbon materials, expanding the photo-responsive range by dye sensitization and modify the dispersion of catalyst in reactive system to improve the reactive interface area between the catalyst and the solution⁴⁻⁸.

In order to accomplish scale-up photocatalytic hydrogen manufacture, easy separation is needed to realize recycle operation of the catalyst, thus using catalyst with a magnetic core to build a composite magnetic photocatalyst is an excellent option for visible-light-driven hydrogen evolution and photo-catalytic decomposition of organics⁹⁻¹². However, developing composite magnetic photocatalyst with HER efficiency is still challenged by limited understanding of the magnetic influence on charge transfer in the composite structure. In fact, it has been found that the magnetic field could affect the redox process of water electrolysis significantly by Lorentz force or Kelvin force¹³⁻¹⁶. An appropriate magnetic field can effectively enhance the electron-transfer rate, promote the reaction of water electrolysis, and even affect the catalytic activity by regulating the surface Spins of catalysts¹⁷. Since the photo-catalytic hydrogen evolution reactions involves the separation and transfer process of photo-generated charges, it is reasonable to speculate that the magnetic field can influence the movement pathway of

photo-generated electrons in a catalyst with a magnetic core, accelerate or retard the H₂ evolution efficiency over these photocatalysts.

Nevertheless, recovering of the magnetic effect on charge transfer in those catalysts has not been fulfilled because of the absence of appropriate catalysts which are simultaneously equipped with a magnetic core, electron in-put molecule and a charge transfer medium. To accomplish this purpose, dye sensitized conjugated compounds, especially the graphene and conductive polymers, could be a nice study model because the conjugated compounds exhibits high conductivity, superior electron mobility and extremely high specific surface area, while the dye offers in-put electron high efficiently. By strategy of assembling the dye sensitized conjugated compounds with a Pt co-catalyst, a dye molecule, as well as a Fe₃O₄ magnetic core to build a magnetic architecture, one can easily study the HER efficiency dependence on magnetic properties under every designed wavelength of irradiation and magnetic field intensity, so as to understand the mechanism of charge movement in those assembled magnetic catalysts.

In this work, we report, for the first time, a new result of the electro-magnetic coupling effects on the dye-sensitized H₂ evolution under the irradiation of visible light ($\lambda \geq 420$ nm). By a dedicated core-shell structural catalyst (Fe₃O₄@PPy@Pt) with ternary functional components, (1) Fe₃O₄ hollow sphere as core to provide the catalyst with super-paramagnetic property and sufficient hydrophilic groups; (2) Polypyrrole (PPy) shell works as the conductive medium to transfer the photo-generated charge, as well as compensates the surface defects of Fe₃O₄ spheres; (3) Pt quantum dots which are dispersed into the PPy shell acts as the co-catalysts. The dependence of charge transfer on intrinsic magnetic field was recovered by such nano-architecture. It is interesting to find that the intrinsic magnetic characteristics of Fe₃O₄@PPy@Pt catalyst remarkable affected their hydrogen generation activity by deflecting the photo-electron transfer in the charge transfer medium. The deflection of photo-electron could be regulated easily by tuning the magnetic nature of photocatalysts.

Fe₃O₄ spheres with different saturation magnetization (*M_s*) was used as the core of Fe₃O₄@PPy@Pt, thus the Fe₃O₄@PPy@Pt ternary photo-catalysts exhibiting different saturation magnetization, as shown in Fig. 1 (a). The photocatalysts are respectively marked as Fe₃O₄@PPy@Pt-A (*M_s*=44.8 emu·g⁻¹), Fe₃O₄@PPy@Pt-B (*M_s*=47.2 emu·g⁻¹), and

$\text{Fe}_3\text{O}_4@\text{PPy}@Pt\text{-C}$ ($M_s=47.2 \text{ emu}\cdot\text{g}^{-1}$). Hydrogen evolutions over different photo-catalysts are measured under visible light irradiation, with Eosin Y dye (EY) as the sensitizer and triethanolamine (TEOA) as the sacrifice reagent. As shown in Fig. 1 (b), in the first run, the $\text{Fe}_3\text{O}_4@\text{PPy}@Pt$ ternary catalysts exhibit higher photo-catalytic activity than the $\text{Fe}_3\text{O}_4@Pt$ catalyst. After 3h photo-catalytic reaction, H_2 evolution over the $\text{Fe}_3\text{O}_4@\text{PPy}@Pt\text{-A}$, $\text{Fe}_3\text{O}_4@\text{PPy}@Pt\text{-B}$, $\text{Fe}_3\text{O}_4@\text{PPy}@Pt\text{-C}$ and $\text{Fe}_3\text{O}_4@\text{PPy}@Pt\text{-D}$ are respectively 3.6, 2.8, 2.0 and 1.8 times higher than that over the $\text{Fe}_3\text{O}_4@Pt$ catalyst. As shown in Fig. 1 (a) and (b), the hydrogen generation over those catalysts is closely related to their saturation magnetization (M_s). H_2 evolution rate over the $\text{Fe}_3\text{O}_4@\text{PPy}@Pt\text{-A}$ and $\text{Fe}_3\text{O}_4@\text{PPy}@Pt\text{-B}$ are respectively 1.8 and 1.4 times higher than that over the $\text{Fe}_3\text{O}_4@\text{PPy}@Pt\text{-C}$ after 3h visible light irradiation.

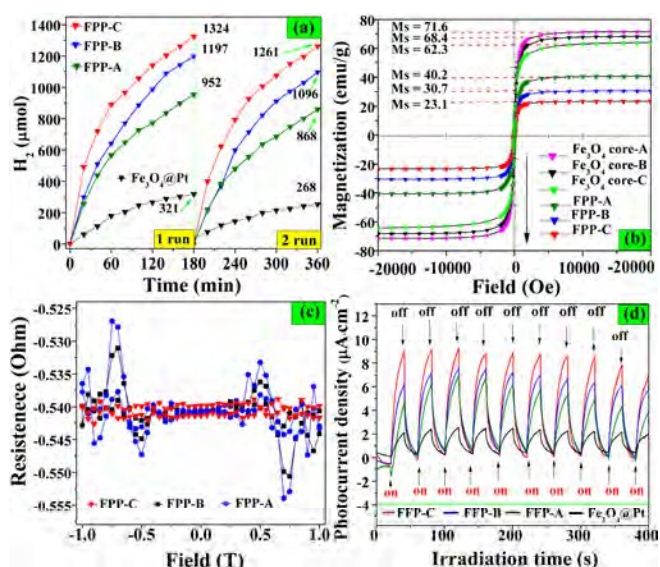


Fig. 1 (a) H_2 evolution ($C_{\text{EY}}=1.0\times 10^{-3} \text{ mol/L}$, $\lambda\geq 420 \text{ nm}$, EY as sensitizer, TEOA as sacrifice reagent) (b) Magnetic hysteresis curves (c) Hall-effect and (d) Transient photocurrent-time profiles of the $\text{Fe}_3\text{O}_4@\text{PPy}@Pt\text{-A}$ (FPP-A), $\text{Fe}_3\text{O}_4@\text{PPy}@Pt\text{-B}$ (FPP-B), and $\text{Fe}_3\text{O}_4@\text{PPy}@Pt\text{-C}$ (FPP-C) photo-catalysts at room temperature

In order to reveal more clues to explain that phenomenon, the Hall effects are measured for those catalysts as the hydrogen evolution reaction is intrinsically an electron transfer process. The catalysts exhibit different response to the external magnetic field which varied from -1.0 to 1.0 Tesla (Fig. 1 (d)). Photo-generated electrons endure higher Lorentz force in $\text{Fe}_3\text{O}_4@\text{PPy}@Pt\text{-A}$ but less Lorentz force in $\text{Fe}_3\text{O}_4@\text{PPy}@Pt\text{-C}$ under magnetic field, because the Hall resistance originates from the Lorentz force acting on the electrons. The charge transfer process for the photo-catalytic HER over $\text{Fe}_3\text{O}_4@\text{PPy}@Pt$ is closely associated to different magnetic-electronic coupling effect caused by the intrinsic magnetic characteristics of catalyst: the electrons in $\text{Fe}_3\text{O}_4@\text{PPy}@Pt\text{-C}$ are less likely to be deflected from their original motion path, whereas the electrons endure more resistance when they transmitted in the $\text{Fe}_3\text{O}_4@\text{PPy}@Pt\text{-A}$. Furthermore, it has been found that the magnetic field could control the space-charge density of electrons beam in materials,

but the maximum current could only be obtained at a suitable optimum magnetic field¹⁸. Fig. 1 (a) and (c) indicates that in the reactive system, the $\text{Fe}_3\text{O}_4@\text{PPy}@Pt\text{-C}$ with weaker Hall effects could provide suitable magnetic nature for enhancing the space-charge density of photo-generated electrons. The electrons then have higher migration rate when they are transferred from the excited dye to Pt active sites for proton. Owing to such effective magnetic-electronic coupling, the $\text{Fe}_3\text{O}_4@\text{PPy}@Pt\text{-C}$ catalysts exhibits better charge-separation efficiency and higher hydrogen production. In addition, even some electrons close to the Pt dots may be deflected from the Pt dots if the Lorentz force is too large, thus further decreasing the proton reduction efficiency over the Pt dots. The Hall effects of ternary catalysts could also be supported by their photo-current (Fig. 1 (d)) that the catalyst with higher M_s value exhibits lower photo-current. $\text{Fe}_3\text{O}_4@Pt$ catalyst is also prepared in this work to compare with the properties of $\text{Fe}_3\text{O}_4@\text{PPy}@Pt$ photo-catalysts. In consistent with the Hall effect results, the $\text{Fe}_3\text{O}_4@\text{PPy}@Pt\text{-A}$ exhibits higher photo-current than the $\text{Fe}_3\text{O}_4@\text{PPy}@Pt\text{-B}$ and $\text{Fe}_3\text{O}_4@\text{PPy}@Pt\text{-C}$ photo-catalysts, indicating larger scale of electron transferring from the PPy to Pt dots inside the PPy layer (Fig. 1 (d)). So the $\text{Fe}_3\text{O}_4@\text{PPy}@Pt\text{-A}$ doesn't exhibit higher photo-catalytic performance though it has stronger magnetic characteristic.

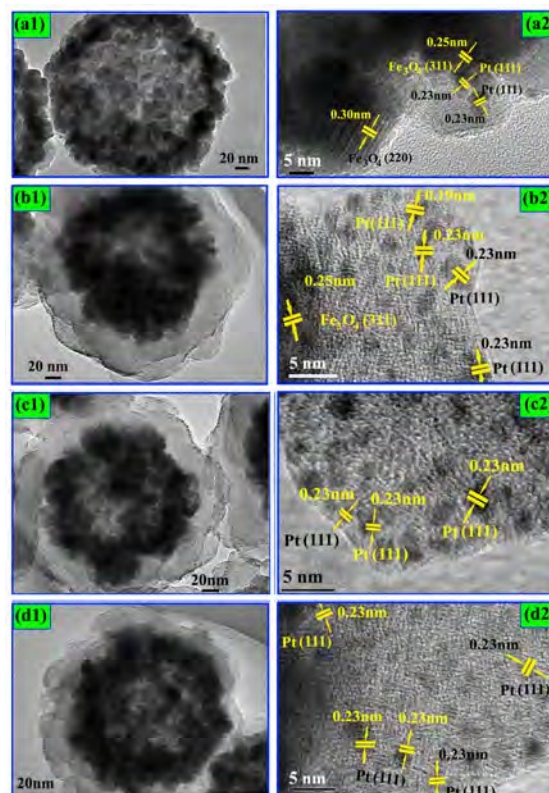


Fig. 2 TEM image and HRTEM image of (a) $\text{Fe}_3\text{O}_4@Pt$, (b) $\text{Fe}_3\text{O}_4@\text{PPy}@Pt\text{-A}$, (c) $\text{Fe}_3\text{O}_4@\text{PPy}@Pt\text{-B}$, and (d) $\text{Fe}_3\text{O}_4@\text{PPy}@Pt\text{-C}$

As shown in Fig. 2 (b1, c1, d1)), Fe_3O_4 hollow microspheres are encapsulated by the polypyrrole (PPy) matrix to build the core-shell structure of photo-catalysts. The Pt nano-dots locate inside the PPy matrix to form a PPy@Pt composite layer. Pt NPs in PPy shell were all synthesized at the same reaction condition by microwave method to make the Pt NPs have approximate

particle size, as shown in HRTEM images (Fig. 2 (b2, c2, d2)). The dots are less than 3 nm and they distributed uniformly in the PPy layer to form a homogeneous metal-polymer network.

It is interesting to find that the Pt dots mainly expose their (111) crystal plane in the PPy layer, as shown in Fig. 2 (b2), (c2), (d2). The oriented growth of Pt nano-crystals has also been found in the graphene-based catalysts¹⁹. It seems that the matrix with abundant delocalized electron (such as the graphene and PPy) could induce the Pt nano-crystals growing preferentially to expose their (111) facets. Compared with the Pt (200) facets, the (111) facets of Pt have higher energy and better photo-catalytic performance for visible-light-driven H₂ evolution^{20,21}.

The HRTEM results are well supported by their XRD patterns (Fig. 3 (a)) and XPS spectra (Fig. 3 (b)). Due to their small size, the diffraction of Pt dots is not obvious in the XRD pattern (Fig. 3 (a)). The Fe₃O₄@PPy@Pt-A, Fe₃O₄@PPy@Pt-B and Fe₃O₄@PPy@Pt-C have approximate Pt 4f binding energy, indicating that the Pt dots in the three catalysts are in similar chemical environments. The Raman spectra reveal more structural information for recovering the magnetic influence on charge transfer in the composite structure (Fig. 3 (c)). The strong band at 1560 cm⁻¹ is assigned to the C=C conjugated bonds, which could provide the PPy layer with abundant delocalized electrons²². C 1s spectra of the catalysts also indicate that the surface of PPy shell are mainly composed of C=C conjugated bonds (Fig. S7). The PPy layer could therefore act as the transfer medium for the photo-generated electrons in dye-sensitized hydrogen evolution reaction. Besides, in this work, the PPy molecules are synthesized by oxidative polymerization of pyrrole molecule. In Fig. 3 (c), the bands at 981 cm⁻¹ is assigned to the bipolaron groups, which clearly confirm the oxidation state of PPy layers²³. The oxidation could further improve the electrical conductivity of PPy layers^{23,24}. Due to effective interfacial electron transfer from the excited EY* to the PPy@Pt shell, the EY luminescence quenched obviously in the presence of ternary catalysts (Fig. 3 (d)).

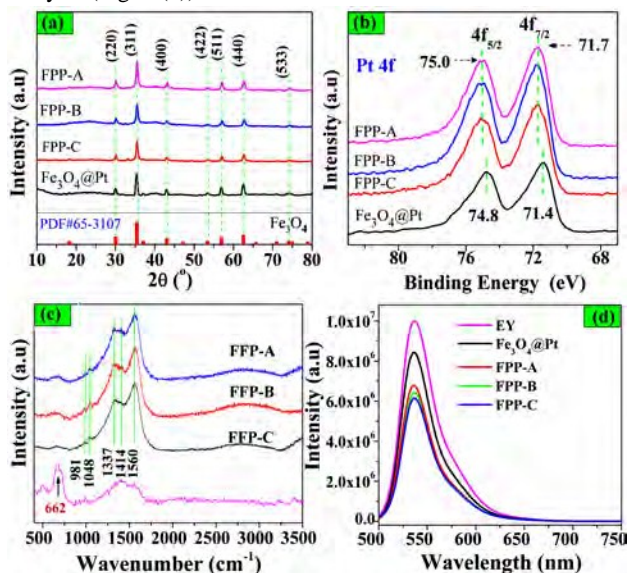
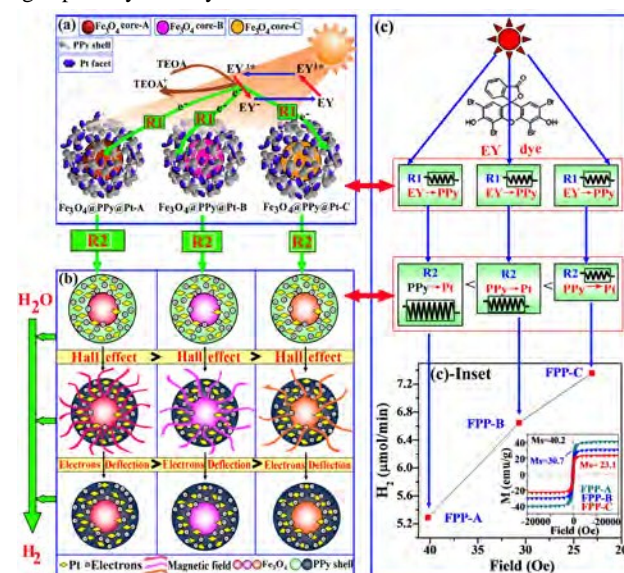


Fig. 3 (a) X-ray diffraction (XRD) patterns (b) Pt 4f spectra, and (c) Raman spectra of Fe₃O₄@Pt, Fe₃O₄@PPy@Pt-A, Fe₃O₄@PPy@Pt-B, and Fe₃O₄@PPy@Pt-C (d) Photo-luminescence of

EY, EY-Fe₃O₄@Pt, EY-Fe₃O₄@PPy@Pt-A (FPP-A), EY-Fe₃O₄@PPy@Pt-B (FPP-B), and EY-Fe₃O₄@PPy@Pt-C (FPP-C)

The PPy@Pt layers play an important role in improving the photo-catalytic activity of the ternary catalysts. The Raman spectra also indicate the PPy@Pt shell could "hide" the Fe₃O₄ core as the Fe-O stretching vibration at 662 cm⁻¹ becomes much weaker than the Fe₃O₄@Pt catalyst (Fig. 3 (c)). It has been found that the surface defects of Fe₃O₄ microspheres could quench the photo-generated electrons and lead to poor hydrogen evolution efficiency of Fe₃O₄@Pt catalyst¹⁸. In consequence, higher catalytic activity of the ternary catalysts could also be attributed to the insulation effect of PPy@Pt layer because the layer can protect the photo-generated electrons from being quenched by the surface defects of Fe₃O₄. In the 2nd run, hydrogen evolution over the Fe₃O₄@PPy@Pt-C catalyst revived to 95.2% while that over the Fe₃O₄@Pt only recovered to 83.5%. Better catalytic stability of the Fe₃O₄@PPy@Pt could also be assigned to the advantages of PPy@Pt layer. The PPy@Pt layer is able to protect the Fe₃O₄ core from acid or alkali corrosion. In addition, the Pt dots could be fixed more stably on the catalysts as they are "grasped" by the PPy shell.



Scheme 1 Charge transfer in the Fe₃O₄@PPy@Pt catalysts (a) **Process 1**, the electron transferring from EY* to PPy layer (Photo-catalytic dye sensitization mechanism); (b) Magnetic disturbance on the electron transferring from PPy to Pt dots (Process 2); (c) Equivalent circuit of photo-catalytic reaction; (Inset of c) Relationship between the saturation magnetization and H₂ evolution

As illustrated in Scheme 1, there exist two electron transfer process during the hydrogen evolution, including the electron transferring from EY* to PPy layer (**Process 1**, EY*→PPy, scheme 1 (a)), and then the electron transferring from the PPy to Pt dots inside the PPy layer (**Process 2**, PPy→Pt, scheme 1 (b)). The photo-currents from the two electron transfer processes will encounter various disturbances, which could be regarded as the electronic resistance for electron transferring. Those resistances are marked as "R1" and "R2" respectively for **Process 1** and

Process 2. As shown in scheme 1 (c), the **R1** and **R2** are connected in series. In Fig. 1 (c), quenching efficiency is 68.5%, 64.5%, and 61.7% for Fe₃O₄@PPy@Pt-A, Fe₃O₄@PPy@Pt-B and Fe₃O₄@PPy@Pt-C catalysts, respectively. The approximate quenching efficiency indicates that in **Process 1**, the three catalysts have approximate electron-transfer efficiency and electrical resistance (**R1**). The variation of photo-currents (Fig. 1 (d)) could be assigned to different electron-transfer efficiency of **Process 2**. In **Process 2**, the photo-generated electrons are transferred from PPy layer to the Pt dots for hydrogen evolution. The photo-catalyst with larger *M_s* value has stronger Hall effects on the photo-generated electrons. Higher Lorentz force could slow down the migration speed of electrons by higher Lorentz force and aggravate the deflection of electrons from their original transfer path, thus depressing the transfer efficiency of electrons. So the photo-currents encounter larger resistance (**R2**) when they move in the Fe₃O₄@PPy@Pt-A and Fe₃O₄@PPy@Pt-B than in the Fe₃O₄@PPy@Pt-C catalysts. In addition, even some electrons close to the Pt dots may be deflected from the Pt dots if the Lorentz force is too large. As a result, intrinsic magnetic characteristic of the photo-catalysts become the key factor in regulating the electron-transfer process and H₂ evolution efficiency.

In summary, super-paramagnetic ternary catalysts have been prepared for dye-sensitized H₂ evolution visible light irradiation ($\lambda \geq 420$ nm). Due to the electron transfer effect of PPy shell, the Fe₃O₄@PPy@Pt catalyst exhibited higher activity for hydrogen evolution than the catalyst without conductive shell. Moreover, this is the first time to build an appropriate architecture to detect whether the magnetic property of the catalysts have effect on their hydrogen generation in the research field of dye-sensitized hydrogen generation. Intrinsic magnetic characteristics of the Fe₃O₄@PPy@Pt catalyst have remarkable effect on the hydrogen generation by accelerating the photo-electron transfer in the charge transfer medium. Only an appropriate magnetic nature can effectively enhance the electron-transfer rate and promote the reaction of water electrolysis. The deflection and migration of photo-electron could be regulated easily by tuning the magnetic nature of photo-catalysts. Such electro-magnetic coupling could effectively enhance the visible-light-driven H₂ evolution over the magnetic photo-catalysts.

This work is supported by the NSF of China (grant no. 21173242 and 21433007) and the 973 Programs of Department of Sciences and Technology of China (2013CB632404, 2012AA051501), respectively.

Notes and references

^aState Key Laboratory for Oxo Synthesis and Selective Oxidation, Lanzhou Institute of Chemical Physics, Chinese Academy of Science, Lanzhou 730000, China

^bUniversity of Chinese Academy of Science, Beijing 10080, China.

^cCollege of Material Engineering, Jinling Institute of technology, Nanjing, China

*Corresponding author: E-mail: gxlu@lzb.ac.cn.

Tel.: +86-931-4968 178. Fax: +86-931-4968 178.

†Electronic Supplementary Information (ESI) available: [details of any supplementary information available should be included here]. See DOI:

- 1 K. J. Maeda, Photochemistry and Photobiology C: Photochemistry Reviews, 2011, **12**, 237.
- 2 Z. Han, R. Eisenberg, Acc. Chem. Res. 2014, **47**, 2537.
- 3 A. Clough, Yoo, J. Mecklenburg, M. Marinescu, S. J. Am. Chem. Soc. 2015, **137**, 118.
- 4 H. Ahmad, Kamarudin, S. K. Minggu, L. J. Kassima, M. Renew. Sust. Energ. Rev. 2015, **43**, 599.
- 5 C. Kong, S. Min, G. Lu, ACS Catal. 2014, **4**, 2763
- 6 Zhang, W. Hong, J. Zheng, J. Huang, Z. Zhou, J. Xu, R. J. Am. Chem. Soc. 2011, **133**, 20680
- 7 Xiang Q. J., Yu J. Phys. Chem. Lett., 2013, **4**, 753.
- 8 Xiang, Q. Yu, J. Jaroniec, M. Chem. Soc. Rev. 2012, **41**, 782.
- 9 D. R. Yang, J. Feng, L.L. Jiang, X. L. Wu, L. Z. Sheng, Y. T. Jiang, T. Wei, Z. J. Fan, Adv. Funct. Mater. 2015, **25**, 7080.
- 10 X. J. Chen, Y. Z. Dai, T. H. Liu, J. Guo, X. Y. Wang, F. F. Li, J. Mol. Catal. A, 2015, **409**, 198.
- 11 S. Li, Y. H. Lin, B. P. Zhang, Y. Wang, C. W. Nan, J. Phys. Chem. C. 2010, **114**, 2903-2908.
- 12 F. Gao, X. Y. Chen, K. B. Yin, S. Dong, Z. F. Ren, F. Yuan, T. Yu, Z. G. Zou, J. Ming, Liu, Adv. Mater. 2007, **19**, 2889.
- 13 P. C. Mondal, C. Fontanesi, D. H. Waldeck, R. Naaman, ACS Nano, 2015, **9**, 3377.
- 14 M. Y. Lin, L. W. Hourng, Int. J. Energy Res. 2014, **38**, 106–116.
- 15 L. M. A. Monzon, J. M. D. Coey, Electrochem. Commun. 2014, **42**, 38.
- 16 J. A. Koza, S. Mühlhoff, P. Zabinski, P. A. Nikrityuk, K. Eckert, M. Uhlemann, A. Gebert, T. Weier, L. Schultz, S. Odenbach, Electrochimica. Acta. 2011, **56**, 2665.
- 17 R. Li, Y. Yang, Ren. Li, Q. W. Chen, ACS Appl. Mater. Interfaces 2015, **7**, 6019.
- 18 L.Brillouin, Phys. Rev. 1945, **67**, 260.
- 19 W. Y. Zhang, C. Kong, G. X. Lu, Chem. Commun., 2015, 51, 10158–10161.
- 20 S. X. Ming, G. Lu, Int. J. Hydrogen Energy. 2012, **37**, 10564.
- 21 E. Cui, G. Lu, J. Phys. Chem. C. 2013, **117**, 26415.
- 22 M. A. Booth, J. Leveneur, A.S. Costa, J. Kennedy, T. S. Jadranka, J. Phys. Chem. C 2012, **116**, 8236.
- 23 Y. Hou, L. Zhang, L. Y. Chen, P. Liu, A. Hirata, M. W. Chen, Phys. Chem. Chem. Phys. 2014, **16**, 3523
- 24 A. Roychowdhury, S. P. Pati, S. Kumar, Mater. Chem. Phys. 2015, **151**, 105.